Sports Medicine and Health Science 7 (2025) 16–27

Contents lists available at ScienceDirect

Sports Medicine and Health Science

journal homepage: www.keaipublishing.com/smhs

Original Article

Sulforaphane, Urolithin A, and ZLN005 induce time-dependent alterations in antioxidant capacity, mitophagy, and mitochondrial biogenesis in muscle cells

Neushaw Moradi, Sabrina Champsi, David A. Hood *

Muscle Health Research Center, School of Kinesiology and Health Science, York University, Toronto, ON, M3J 1P3, Canada

ARTICLE INFO

Keywords:
Mitochondria
Skeletal muscle
Nrf-2
AMPK
Exercise mimetic

ABSTRACT

Efficient signal transduction that mediates mitochondrial turnover is a strong determinant of metabolic health in skeletal muscle. Of these pathways, our focus was aimed towards the enhancement of antioxidant capacity, mitophagy, and mitochondrial biogenesis. While physical activity is an excellent inducer of mitochondrial turnover, its ability to ubiquitously activate and enhance mitochondrial turnover prevents definitive differentiation of the contribution made by each pathway. Therefore, we employed three agents, Sulforaphane (SFN), Urolithin A (UroA), and ZLN005 (ZLN), which are activators of important biological markers involved in antioxidant signaling, mitophagy, and biogenesis, respectively. We investigated the time-dependent changes in proteins related to each mechanism in C2C12 myotubes. SFN treatment resulted in increased nuclear localization of the transcription factor Nuclear factor (erythroid-derived 2)-like 2 (Nrf-2) after 4 hour (h), with subsequent 2-fold increases in the antioxidant enzymes Nicotinamide Quinone Oxidoreductase 1 (NQO1) and Heme-Oxygenase-1 (HO-1) by 24 h and 48 h. Mitochondrial respiration and ATP production were significantly increased by both 24 h and 48 h. UroA showed a 2-fold increase in AMP-activated Protein Kinase (AMPK) after 4 h, which led to a modest 30% increase in whole cell mitophagy markers p62 and LC3, after 48 h. This was accompanied by a reduction in cellular Reactive Oxygen Species (ROS), detected with the CellROX Green reagent. Mitophagy flux measurements showed mitophagy activation as both LC3-II and p62 flux increased with UroA at 24-h and 48-h time points, respectively. Finally, AMPK activation was observed by 4 h, in addition to a 2-fold increase in Mitochondrial Transcription Factor A (TFAM) promoter activity by 24 h of ZLN treatment following transient transfection of a TFAM promoter-luciferase construct. Mitochondrial respiration and ATP production were enhanced by 24 h. Our results suggest that early time points of treatment increase upstream pathway activity, whereas later time points represent the increased phenotypic expression of related downstream markers. Our findings suggest that the spatiotemporal progression of these mechanisms following drug treatment is another important factor to consider when examining subcellular changes towards mitochondrial turnover in muscle.

1. Introduction

Mitochondria fuel energy-dependent processes in the cell and their regulation and function depend on the cellular response to signal transduction events to maintain cellular homeostasis. Metabolic derangements in skeletal muscle, borne of aging, disuse, denervation, or disease[1] can be caused by impairments in intrinsic signal transduction pathways that typically take place in healthy muscle.[2,3] Despite the activation of mechanisms dedicated to mitochondrial turnover with exercise[4–7] full restoration of optimal organelle function can be limited. [2] While exercise is now known to effectively refresh the mitochondrial pool, the redundancy of multiple pathway activation can blur the unique character of the individual pathways that contribute to an improved metabolic outcome. In this respect, nutraceutical and pharmaceutical agents that have been developed over time for therapeutic intervention can prove useful in identifying the activation of important cellular mechanisms to illuminate their unique contributions to maintaining or improving mitochondrial homeostasis.

Of interest in this respect are the agents that typically increase the drive for mitochondrial biogenesis, mitochondrial autophagy (hereafter referred to as mitophagy), and antioxidant capacity, likely in a time-

* Corresponding author. Muscle Health Research Centre, School of Kinesiology and Health Science York University, 4700 Keele St, Toronto, ON, M3J 1P3, Canada.
E-mail address: dhood@yorku.ca (D.A. Hood).

https://doi.org/10.1016/j.smhs.2024.03.011
Received 4 January 2024; Received in revised form 14 February 2024; Accepted 29 March 2024
Available online 4 April 2024

List of abreviations

SFN	Sulforaphane
UroA/UA	UrolithinA
Nrf-2	Nuclear factor (erythroid-derived 2)-like 2
ARE	Antioxidant Response Element
NQO1	Nicotinamide Quinone Oxidoreductase 1
HO-1	Heme-Oxygenase-1
ATP	Adenosine triphosphate
AMPK	AMP-activated Protein Kinase
P62	Sequestosome-1 (SQSTM1)
LC3	Microtubule-associated proteins 1A/1B Light Chain 3A
ROS	Reactive Oxygen Species
TFAM	Mitochondrial Transcription Factor A
Keap1	Kelch-like ECH-associated protein
PGC-1α	Peroxisome proliferator-activated receptor (PPAR) γ coactivator 1 alpha
BafA	Bafilomycin A
IDP	Intrinsically Disordered Proteins
NRF1	Nuclear Respiratory Factor-1
NRF2	Nuclear Respiratory Factor-2
NuGEMPs	Nuclear Gene-encoding Mitochondrial Proteins
COX IV	Cytochrome oxidase subunit IV
COX I	Cytochrome oxidase subunit I
VDAC	Voltage Dependent Anion Channel
H2B	Histone H2B
pGL3	promoter-reporter Luciferase
EV	Empty Vector
FITC	Fluorescein isothiocyanate
OCR	Oxygen Consumption Rate

dependent manner. Data mining revealed three agents that have gained considerable traction in the literature and that are relevant to our experimental goals. These include the two nutraceutical agents Sulforaphane (SFN)[8–10] and Urolithin A (UroA),[11–15] alongside the third synthetic small molecule, ZLN005.[16,17]

SFN is a potent activator of the Nuclear factor (erythroid-derived 2)-like 2 (Nrf-2)- Kelch-like ECH-associated protein (Keap1)-Antioxidant Response Element (ARE) antioxidant axis which governs the transcriptional regulation of phase II detoxification enzymes for cytoprotection. Available in cruciferous vegetables, this isothiocyanate and phytochemical is deemed to be one of the most important potent cellular defence compounds readily available in natural diets. While its therapeutic application originated in neurological disease and chemoprevention,[18,19] SFN has also been positioned as a metabolic preserver in skeletal muscle.[8,20] SFN appears to be highly specific to Nrf-2-mediated signaling, which can uncover the pathway-specific benefits towards mitochondrial preservation.

UroA has gained a considerable reputation based on *in vitro* studies as well as those conducted in human subjects[11–15] and has been identified as a mitophagy activator. This ellagitannin has been reported to restore mitophagy starting at the upstream activating kinase, AMP-activated Protein Kinase (AMPK), thus preventing the accumulation of unhealthy mitochondria in the cell.[11] It gained its fame in the literature as a useful agent that restores mitochondrial clearance in aged skeletal muscle without direct targeting of mitochondrial biogenesis, thus promoting healthy aging of the cell. However, the data supporting the direct effects of UroA on mitophagy in muscle are not overly convincing, upon close inspection. Therefore, our goal was to characterize this agent by investigating its time-dependent ability to induce mitophagy in our *in vitro* model of skeletal muscle myotubes.

The small synthetic molecule, ZLN005 has been reported to activate Peroxisome proliferator-activated receptor (PPAR) γ coactivator 1 alpha (PGC-1α) and relieve some of the symptoms of insulin resistance.[16] ZLN005 appears to stimulate the nuclear translocation of PGC-1α and therefore may upregulate the drive for mitochondrial biogenesis.[21] For this reason, we hypothesized that it would be a suitable candidate as an activator of the expansion of the mitochondrial reticulum in skeletal muscle.

Countless pharmacological agents have been considered as research-based interventions that improve skeletal muscle health. Over time, continued elucidation around skeletal muscle cellular modulation adds information to the pharmacological blueprints that can refine drug function and improve their metabolic mimicry. While we limit our study to these three agents, we wished to 1) examine the integrity of these agents as activators of divergent, yet cooperative mitochondria-related pathways in C2C12 myotubes, and 2) expand on the characterization of these mechanisms and their unique cascade by examining the dose- and time-dependent changes of their relevant biochemical effects.

2. Materials & methods

2.1. Mammalian cell culture and drug treatments

C2C12 murine myoblasts were seeded on six-well culture dishes (Fisher Scientific) in Dulbecco's modified Eagle's medium (DMEM) supplemented with 10% fetal bovine serum (FBS) and 1% penicillin-streptomycin (P/S). At 80%–90% confluency, differentiation into myotubes was induced by switching the medium to DMEM supplemented with 5% heat-inactivated horse serum (HS) and 1% P/S. Between day 5–6 of differentiation, cells were treated with vehicle (DMSO) or differing concentrations of Sulforaphane (5 μM, 10 μM) (MedChemExpress), Urolithin A (20 μM, 50 μM, or 100 μM) (MedChemExpress), or ZLN005 (10 μM, 20 μM). Drug treatments were followed by 4 h, 24 h, or 48 h of incubation time to examine their time-dependent effects.

2.2. Immunoblotting

Cells were lysed and proteins were extracted with 1 × passive lysis buffer diluted from a 5 × stock (Promega), 1 x phosphatase cocktails, and 1 × protease inhibitor (Millipore-Sigma). Protein concentrations for each sample were determined via Bradford concentration assay. Protein samples (15–25 μg) were then loaded and separated on SDS-PAGE gels followed by transfer to nitrocellulose membranes. Membranes were then washed in Ponceau stain and cut at an appropriate range according to the molecular weight of each protein of interest. Each blot was later blocked using 5% milk or 5% bovine serum albumin at room temperature for approximately 1 h. Western blot analyses were performed using primary antibodies against Nrf-2 (ProteinTech), Keap1 (ProteinTech), Phospho-AMPK (Cell Signaling), AMPK (Cell Signaling), LC3 A/B (Cell Signaling), GAPDH (Abcam), SQSTM1/p62 (Abcam), PGC-1α (Millipore-Sigma), H2B (Cell Signaling), Luciferase (Millipore-Sigma), COX IV (Abcam), and α-tubulin (Calbiochem). Blots were imaged using ECL Clarity Substrates (BIO-RAD), Invitrogen Imaging instrument, and quantification takes place using the ImageJ software. Values were normalized to each protein's corresponding loading control.

2.3. Nuclear-cytoplasmic fractionation

Nuclear and cytoplasmic fractions were isolated as described by Bhattacharya et al.[22] Cells were harvested in cytoplasmic buffer containing 0.2% phosphatase and protease inhibitors. Samples were incubated on ice for 5 minutes (min) and centrifuged at 2 500 × *g* for 5 min.

The supernatant fraction of each sample was collected as the cytoplasmic fraction. Following this, each nuclear pellet was washed and resuspended with cytoplasmic buffer, followed by 3 min of rocking in 4 °C, and 3 min centrifugation at 3 200 × *g*. The wash step was repeated 10–12 times to ensure thorough clearance of cytoplasmic fraction from the nuclear pellet. Then, the pellet for each sample was resuspended in nuclear buffer, and 0.15 unit/μL of Benzonase nuclease was added to each sample. The protein concentration was established via Bradford concentration assay followed by examination of content for each fraction through immunoblot analysis.

2.4. Cytoplasmic-mitochondrial fractionation

We isolated cytoplasmic and mitochondrial fractions to examine the integrity of UroA as a mitophagy activator. Prior to fractionation, cells were co-treated with UroA and Bafilomycin A, an inhibitor of autophagosome-lysosome fusion.[23] Following 24 or 48 h of treatment, cells were washed and scraped with ice cold 1 x PBS. They then underwent centrifugation at 1 400 × *g* for 5 min. The supernatant fraction was then aspirated, and the cells were resuspended with resuspension buffer with an arbitrary volume that is roughly 3–4 times the pellet size. They were then transferred to smaller Eppendorf tubes for better handling and centrifugation. Cells were incubated on ice for 5 min prior to sonication. The sonication protocol involved 2–3 repetitions of 3–5 seconds(s) sonication, with a minimum of 10 s rest between repetitions. Cells were centrifuged at 1 000 × *g* for 10 min in 4 °C. The supernate was collected and transferred to new tubes, and the pellet was discarded. It was then centrifuged at 14 000 × *g* for 15 min at 4 °C. The supernate following this was collected and stored at −80 °C until use, as the cytoplasmic fraction. Approximately 100 μL of resuspension buffer was then added to the remnant pellet and resuspended prior to two more centrifugation periods at 14 000 × *g* for 10 min, with new resuspension buffer added between each spin. The supernate was then discarded, and 25–50 μL of resuspension buffer was added to the pellet to be resuspended. Samples were freeze-thawed on dry ice 2–3 times. Each sample was then stored at −80 °C until use. The protein concentration was established via Bradford concentration assay followed by examination of content for each fraction through immunoblot analysis.

2.5. Promoter-reporter transient transfections

A promoter-reporter Luciferase (pGL3) construct for TFAM was used to assess promoter activity for its transcription[23] as an indirect indication of activated and nuclear-localized PGC-1α following ZLN treatment. C2C12 myoblasts were transiently transfected at approximately 50% confluency with Lipofectamine 2000 and a pGL3-empty vector (EV), or the full TFAM promoter construct located upstream of a luciferase reporter sequence in minimal DMEM (media that does not contain antibiotics or serum). Cells were incubated in this medium for 16–18 h and then switched to regular growth media, as described.[23] Once 80% confluency was reached, cells were differentiated for 5–6 days prior to desired treatments.

2.6. Mitochondrial respiration using seahorse analyses

Approximately 2 500 cells/well were seeded and grown in Seahorse 96-well plates and differentiated for 5 days as described above. On day 6, myotubes were treated with either SFN, UroA or ZLN005 for 24 h and 48 h with the corresponding vehicle for each time point. Media was replenished with either vehicle or drug at 24-h for 48-h analysis. The Seahorse XF96 Mito Stress Test Kit (Agilent, Biosciences, 103015-100; Seahorse XFe96 Analyzer, Agilent Biosciences) was performed according to manufacturer's instructions. Following the assay, myotubes were stained with 100 nM MitoTracker Green (ThermoFisher, 62249) and 10 μM Hoechst (ThermoFisher, M7514) in phenol free media for 30 min at 37 °C. Fluorescence was measured using the Cytation5 plate reader (BioTek Instruments), and all Oxygen Consumption Rates (OCR) were normalized to mitochondria and nuclei with MitoTracker Green and Hoechst respectively to determine OCR per mitochondria per cell. Seahorse assay results were analyzed using the XF Wave software (Agilent, Biosciences).

2.7. Flow cytometry

All flow cytometry experiments were completed using the Beckman Coulter CytoFlex utilizing the CytExpert software. Myoblasts were seeded in 6-well plates and differentiated as described above. Myotubes were treated with either vehicle or 50 μM UroA for 4, 24 or 48 h. Following treatment, myotubes were stained with 100 nM CellROX™ Green Reagent (ThermoFisher, C10444) in phenol free media for 30 min at 37 °C. Following incubation, myotubes were washed with ice cold PBS then trypsinized for 5 min at 37 °C. Cells were scraped then placed in Eppendorf tubes before being centrifuged at 1 000 × *g* for 4 min. Each cellular pellet was resuspended in ice cold PBS and analyzed. CellROX™ Green was gated using the FITC (Fluorescein isothiocyanate) channel.

2.8. Statistical analysis

All data were analyzed using Prism software (GraphPad) and were summarized as Means + *S.E.M.* Raw data were analyzed using a paired *t*-test to assess the differences between control and treated cells. One-way ANOVAs were used to assess the effect of time or concentration with treatments for the 4- and 24-h time points. Two-way ANOVAs were used to assess the 48-h time point. Statistical significance was set at $p < 0.05$.

3. Results

3.1. Sulforaphane increases Nrf-2 nuclear localization at 4 h, but the effect dissipates by 24 h and 48 h

SFN is recognized for its role as an activator of the Nrf-2-Keap1 pathway. We used 5 μM and 10 μM of SFN to investigate changes at 4-, 24-, and 48-h time points in C2C12 myotubes. We hypothesized that an early time point may demonstrate early activation of the Nrf-2 transcription factor as it represents one of the initiating steps in this antioxidant axis, while later time points may show increased downstream antioxidant proteins borne of Nrf-2-ARE-mediated antioxidant activation.

A 2-fold elevation in Nrf-2 protein content was observed after 4 h ($p < 0.05$) of SFN treatment at 10 μM concentration, an approximate 1.5-fold increase by 24 h, but this effect dissipated at 48 h (Fig. 1A). A main effect of time was observed, demonstrating the progressive restoration of Nrf-2 content back to control levels (Fig. 1A). The corresponding fold-change measured as the ratio of SFN over vehicle data was calculated to better observe this progression over time (Fig. 1C). Conversely, changes to Keap1 showed a trending effect of time, where 24 h of treatment showed decreased content that was restored after 48 h ($p = 0.0558$; Fig. 1B–D). To examine Nrf-2 nuclear localization with SFN, we used cytoplasmic and nuclear fractions of C2C12 myotubes treated with 5 μM and 10 μM concentrations after 4 h. A near 2-fold elevation in Nrf-2 nuclear content, compared to vehicle-treated cells occurred with SFN at 5 μM ($p < 0.05$), confirming increased localization of the transcription factor to the nucleus (Fig. 1E).

3.2. Sulforaphane induces time-dependent changes to antioxidant enzymes commonly related to the Nrf-2-ARE axis

Both concentrations of SFN were used to test the changes in protein content of Nicotinamide Quinone Oxidoreductase 1 (NQO1) and Heme-Oxygenase-1 (HO-1) antioxidant enzymes (Fig. 2A and B). While NQO1 protein showed no change with SFN at either concentration (Fig. 2A), HO-1 exhibited an early and marked elevation of 50%–60% with respect

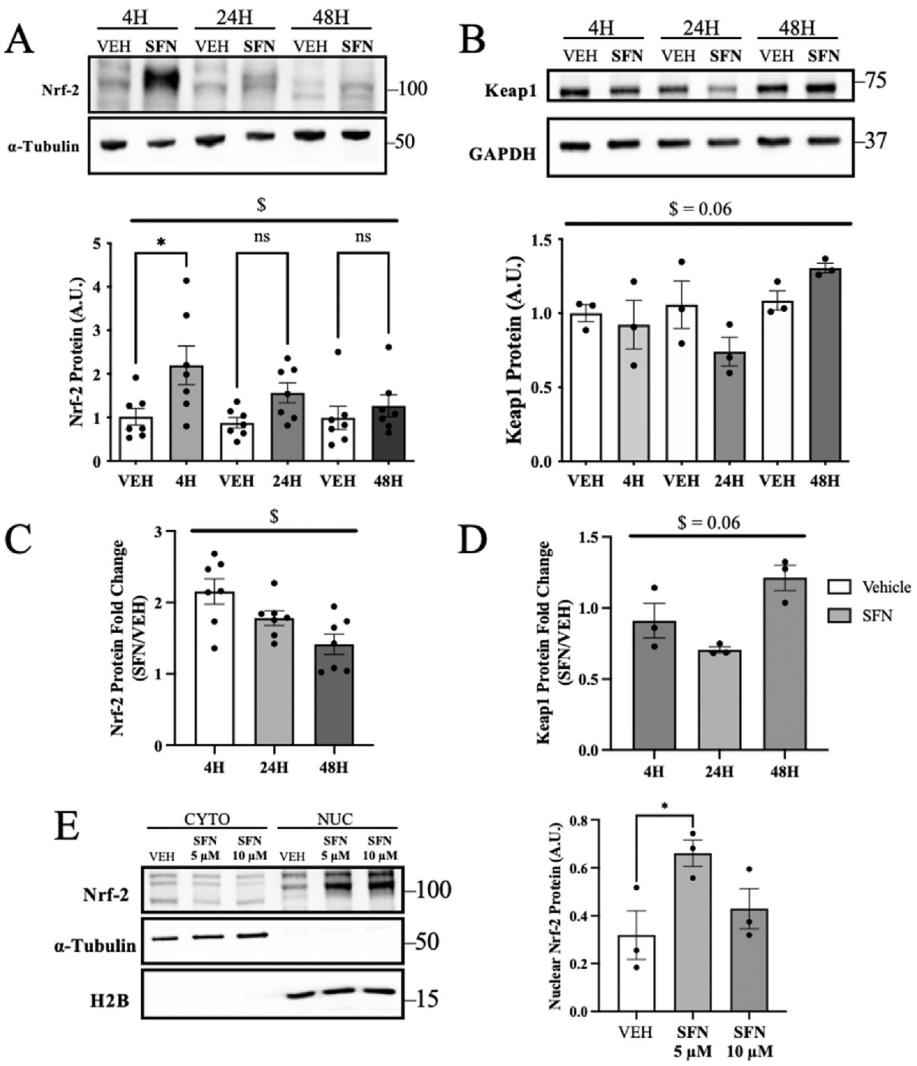

Fig. 1. Upstream protein markers observed in the Nrf-2-ARE antioxidant pathway following Sulforaphane treatment. A: Progression of Nrf-2 content with time at 10 μM SFN concentration at each time point ($n = 7$). One-way ANOVA, $\$p < 0.05$, main effect of time; $^*p < 0.05$, treatment vs. vehicle. B: Progression of Keap1 content with time at 10 μM SFN concentration at each time point ($n = 3$) One-way ANOVA. C, D: Fold-change (SFN/VEH) for Nrf-2 and Keap1 proteins, respectively, at each time point, related to panels A and B, respectively; $\$ p < 0.05$, main effect of time. E: Nuclear localization analysis using nuclear and cytosolic fractionation observing Nrf-2 protein content with SFN treatment ($n = 3$); $^*p < 0.05$, treatment vs. vehicle. *VEH,* Vehicle-treated cells with DMSO*; SFN,* Sulforaphane-treated cells. *Nrf-2,* Nuclear factor (erythroid-derived 2)-like 2. *ARE,* Antioxidant Response Element. *Keap1,* Kelch-like ECH-associated protein. Values are means ± *SEM*.

to both concentrations and this was maintained throughout the remaining time points (Fig. 2B). NQO1 was increased by 2-fold at 24 h, which was maintained at 48 h, with a main effect of treatment and time ($p < 0.05$; Fig. 2A). Thus, SFN-mediated activation of the Nrf-2-Keap1-ARE pathway was evident, with time-dependent changes in the effects of proteins, as well as in specific downstream targets.

3.3. Sulforaphane increases mitochondrial respiration and content by 48 h

Mitochondrial respiration was assessed using Seahorse, utilizing 10 μM SFN for all experiments. Basal respiration, maximal respiration, spare respiratory capacity, and ATP production were all enhanced as early as 24 h (Fig. 3B–F). However, changes in mitochondrial content were not observed until 48 h, where an approximate 40% increase occurred with either concentration ($p < 0.05$; Fig. 3A), indicating there were no stark differences between SFN concentrations during the time points where elevations in content were observed.

3.4. Urolithin A modestly increases AMPK-mediated mitophagy markers while markedly increasing mitophagy flux

UroA has been reported to be an activator of the mitophagy pathway. To evaluate this possibility, we used 20, 50, or 100 μM concentrations of UroA to investigate changes in proteins relevant to mitophagy and autophagy at 4-, 24-, and 48-h time points. At 4 h of treatment, a 2-fold increase ($p < 0.05$) in activated AMPK, represented as the ratio of phosphorylated AMPK over total AMPK, was observed at 50 μM UroA concentration (Fig. 4A). However, this effect was no longer evident at longer time points, indicating its transient activation (Fig. 4A). On the other hand, p62 and total LC3, measured as the ratio LC3-II/I, showed a main effect of treatment relative to control after 48 h in whole cell lysates ($p < 0.05$; Fig. 4B and C). Interestingly, this was accompanied by a reduction in cellular ROS by 24 h ($p < 0.01$; Fig. 4D), possibly indicating induction of mitophagy to assist in the removal of dysfunctional mitochondria.

To fortify whether UroA could activate mitophagy, we measured mitophagy flux. Western blots of cytoplasmic and mitochondrial fractions probing for p62 and total LC3 were conducted following 24 and 48 h of UroA-Bafilomycin A (BafA) or vehicle treatment (Fig. 5A and B). The ratio of LC3-II/I for each condition at 24 and 48 h showed a main effect of UroA, as well as an interaction effect between time, UroA, and BafA (Fig. 5C). A marked 50% increase in mitophagy flux was evident at 24 h (Fig. 5D). Interestingly, p62 mitochondrial localization was increased by BafA and UroA, at 24 and 48 h ($p < 0.05$; Fig. 5E). However, the increase in p62 flux as a result of UroA treatment was only apparent after 48 h (Fig. 5F). Overall, the data show modest increases in whole cell mitophagy markers, and considerable increases in mitophagy flux between 24 and 48 h of treatment.

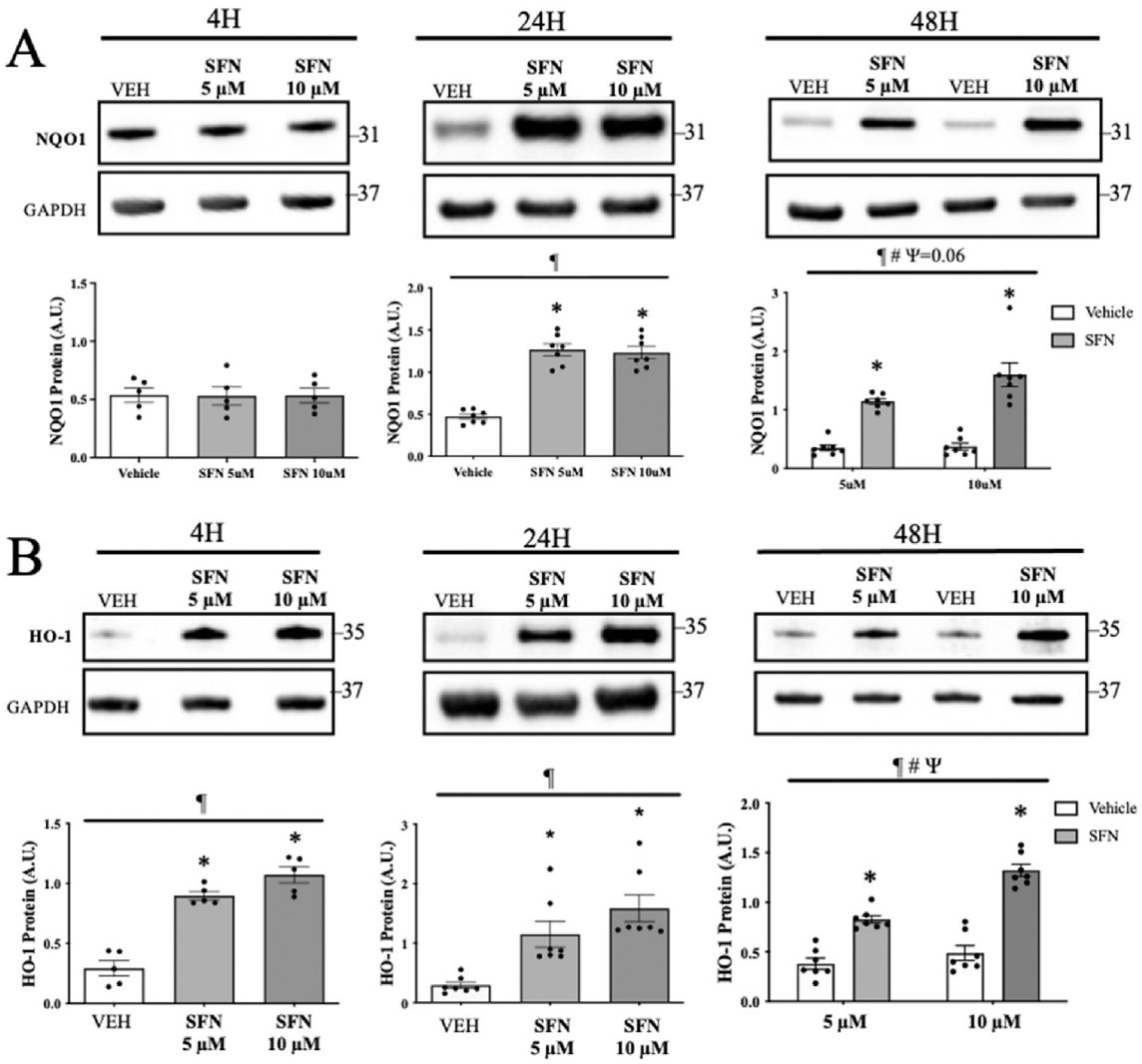

Fig. 2. Downstream protein markers observed in Nrf-2-ARE antioxidant pathway following Sulforaphane treatment. Content of downstream proteins NQO1 (A) and HO-1 (B) respectively, typically targeted by Nrf-2-ARE mechanism, following each given time point. Time points 4 h ($n = 5$) and 24 h ($n = 7$) underwent one-way ANOVA and 48 h ($n = 7$) underwent two-way ANOVA, ¶$p < 0.05$, main effect of treatment relative to control; #$p < 0.05$, main effect of concentration; Ψ$p < 0.05$, interaction effect between treatment and concentration; *$p < 0.05$, treatment vs. vehicle. *VEH,* Vehicle-treated cells with DMSO*; SFN,* Sulforaphane-treated cells. *Nrf-2,* Nuclear factor (erythroid-derived 2)-like 2. *ARE,* Antioxidant Response Element. *NQO1*, Nicotinamide Quinone Oxidoreductase 1. *HO-1*, Heme-Oxygenase-1. Values are means ± *SEM*.

3.5. ZLN005 increases AMPK activation, TFAM promoter activity, and mitochondrial respiration

ZLN005 has been reported to increase PGC-1α expression, and therefore we speculated that it could induce mitochondrial biogenesis in C2C12 myotubes. We used 10 or 20 μM concentrations to investigate changes in relevant proteins at 24 and 48 h of treatment. In contrast to previous reports,[16,17] we were unable to confirm that ZLN could increase PGC-1α or promote its nuclear localization at either 24 or 48 h (Fig. 6C). However, both concentrations of ZLN enhanced AMPK activation by 4 h which dissipated by 24 h and 48 h, demonstrating an alternative mechanism of ZLN mediated mitochondrial biogenesis (Fig. 6A and B). This was fortified when investigating the promoter activity of TFAM, following Lipofectamine-mediated transfection of a TFAM promoter-luciferase reporter. After promoter transfection and 24 h of ZLN treatment, a two-way ANOVA ($p < 0.05$) revealed a main effect of both promoter and ZLN, as well as an interaction effect. This significance is attributed to the approximately 40% increase in luciferase protein content compared to that of empty vector-treated cells (Fig. 6D). Additionally, luciferase content corrected for Empty Vector results (PROM-EV) fortify the 40% increase that was observed (Fig. 6D). Mitochondrial respiration analysis demonstrated a moderate increase in basal respiration, maximal respiration, spare respiratory and ATP production by 24 h (Fig. 6E–I). However, there was a stark decline in these parameters by 48 h. Overall, while conclusive evidence that ZLN005 is an activator of mitochondrial biogenesis in C2C12 myotubes has yet to be uncovered, we believe that it shows promise as a result of its capacity to increase mitochondrial respiration, TFAM promoter activity, and AMPK activation in a time-dependent manner.

4. Discussion

Mitochondria are vital for their roles in the maintenance of cellular metabolic homeostasis. The rationale for this study was to add to the continued characterization of important mechanisms dedicated to refreshing the mitochondrial pool in skeletal muscle cells by examining the time-dependent changes in three important arcs of mitochondrial phenotype. Those pertaining the present study include mitochondrial biogenesis, mitophagy, and antioxidant capacity.[1,24] Unlike the ubiquitous capacity for exercise to simultaneously activate these pathways, we

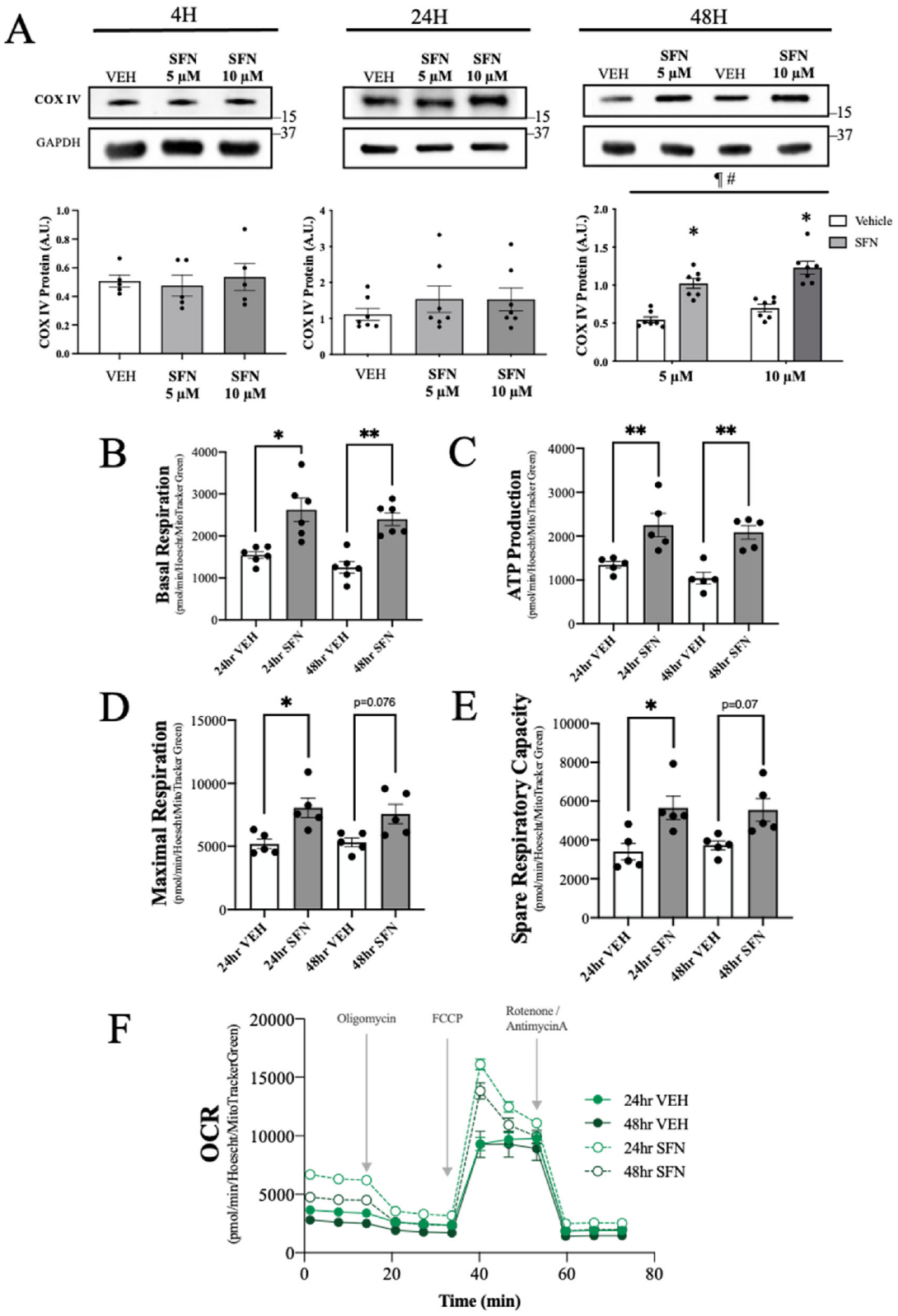

Fig. 3. Mitochondrial content and respiration measurements following Sulforaphane treatment. COX IV protein content following 10 µM SFN treatment following each given timepoint. Time points 4 h ($n = 5$) and 24 h ($n = 7$) underwent one-way ANOVA and 48 h ($n = 7$) underwent two-way ANOVA. ¶$p < 0.05$, main effect of treatment relative to control; #$p < 0.05$, main effect of concentration; *$p < 0.05$, treatment vs. vehicle. (A). Oxygen consumption rates of treatment and vehicle during basal respiration (B), ATP production (C), maximal respiration (D) and spare respiratory capacity (E) using seahorse and correcting for nuclear and mitochondrial content to obtain a measure of mitochondrial function per cell ($n = 11$). 24 h and 48 h Seahorse data underwent one-way ANOVA; *$p < 0.05$, **$p < 0.01$, treatment vs vehicle. Representative oxygen consumption tracing (F). *VEH,* Vehicle-treated cells with DMSO*; SFN,* Sulforaphane-treated cells. *COX IV*, Cytochrome oxidase subunit IV; *OCR,* Oxygen Consumption Rate. Values are means ± *SEM*.

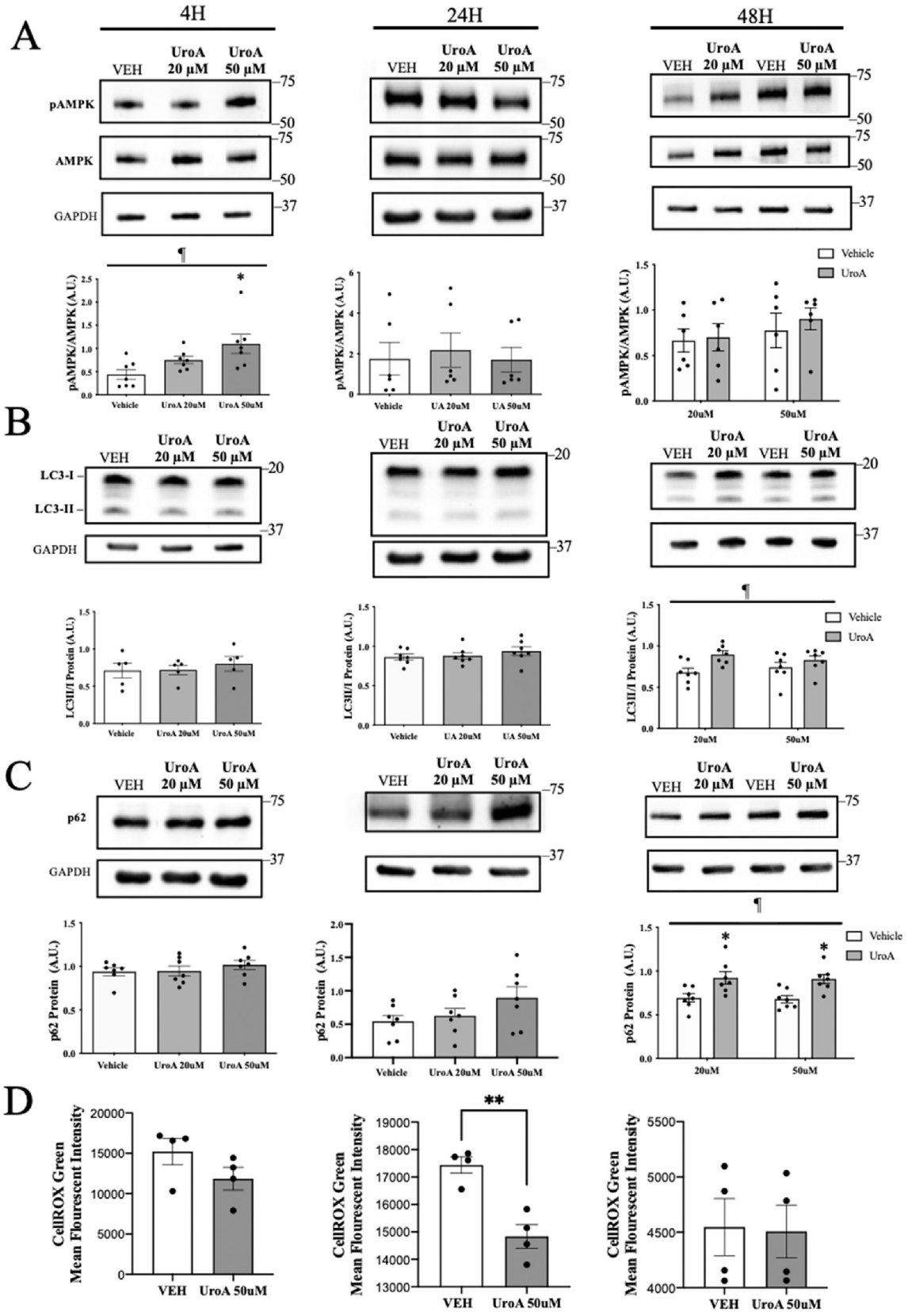

Fig. 4. Whole cell mitophagy markers and ROS following Urolithin A treatment. Content of downstream proteins AMPK (A), LC3 (B), and p62 (C) respectively, typically involved in mitophagy mechanism, and cellular ROS detected with the CellROX Green reagent following each given time point (D). Time points 4 h and 24 h underwent one-way ANOVA and 48 h underwent two-way ANOVA for the evaluation of mitophagy related proteins. CellROX Green data underwent an unpaired *t*-test for each time point. ¶$p < 0.05$, main effect of treatment relative to control; *$p < 0.05$, **$p < 0.01$, treatment vs. vehicle. *VEH,* Vehicle-treated cells with DMSO*; UroA,* Urolithin-A-treated cells. *AMPK,* AMP-activated Protein Kinase. *LC3,* Microtubule-associated proteins 1A/1B Light Chain 3A. Values are means ± *SEM*.

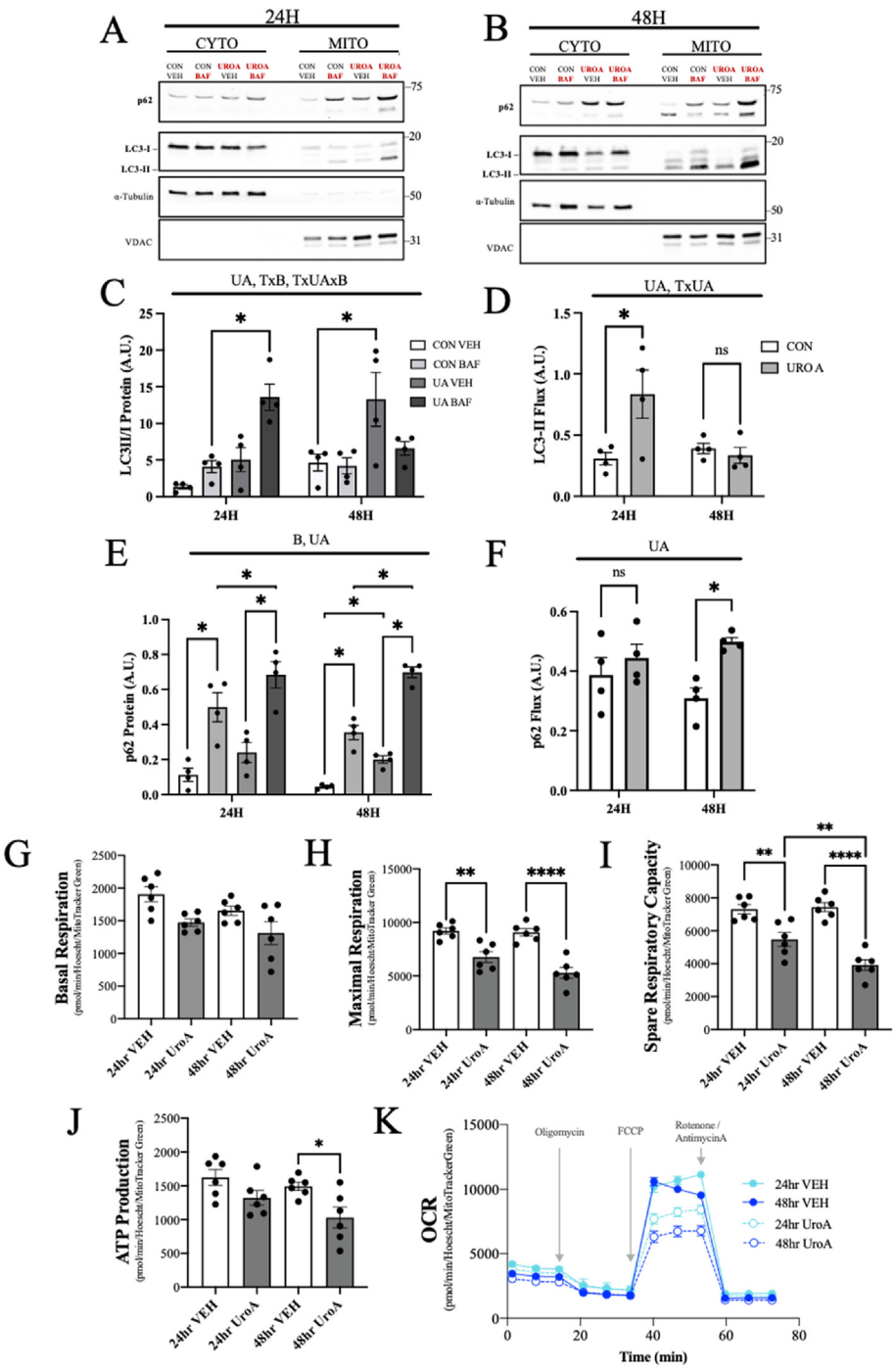

Fig. 5. Mitophagy flux following Urolithin A and Bafilomycin A co-treatment. Western blots showing cytoplasmic and mitochondrial fractions following UroA (100 μM) and BafA (12 nM) co-treatment to assess mitochondrial targeting after 24 h (A) ($n = 4$), and 48 h (B) ($n = 4$). Mitophagy markers p62 (C) and LC3II/I ratio (D) alongside their respective p62 (E) and LC3-II (F) flux measurements were assessed to determine mitochondrial targeting for degradation ($n = 4$) C, D: Three-way ANOVA between Time (T), Bafilomycin A (B), Urolithin A (UA) and E, F: Two-way ANOVA between Time (T) and Urolithin A (UA). C–E: Main effects at $p < 0.05$; 'x' between conditions signifies interaction effects. *$p < 0.05$, *t*-tests between indicated conditions. *UroA,* Urolithin-A-treated cells. *Baf A,* Bafilomycin A; *AMPK,* AMP-activated Protein Kinase. *LC3,* Microtubule-associated proteins 1A/1B Light Chain 3A; *VDAC,* Voltage Dependent Anion Channel; *OCR,* Oxygen Consumption Rate. Values are means ± *SEM*.

used three different agents that have been reported to activate each associated pathway separately in order to differentiate between the cascading events that take place for organelle turnover during exercise.

Previous reports have found that SFN activated antioxidant enzymes through the Nrf-2/Keap1/ARE pathway,[8–10] leading to important findings with chemoprevention and improvements to health within neurodegenerative diseases. Briefly, SFN aids in the cysteine modification of multiple residues on the Keap1 homodimer, which enables nascent Nrf-2 to bypass its negative regulation and accumulate in the nucleus. Nuclear Nrf-2 then binds to ARE enhancer sequences on the promoter region of multiple target genes such as NQO1 and HO-1, resulting in their transcription.[7] A growing body of literature has documented the use of SFN as it improves insulin sensitivity and frailty with aging in skeletal muscle.[20]

To explore the time-dependent changes in SFN-mediated Nrf-2-ARE activation in our *in vitro* model of skeletal muscle, we treated C2C12 myotubes with two concentrations of SFN and analyzed markers of the Nrf-2-ARE mechanism after 4, 24, and 48 h. Not only does SFN increase Nrf-2 protein content, but it also permits nuclear localization of the transcription factor, which likely initiates the cascading events for Nrf-2/ARE-mediated antioxidant capacity. With respect to Keap1 content, we did not expect any reciprocal events where an upregulation of nascent Nrf-2 would result in a downregulation of Keap1. However, we observed a main effect of time, where reductions in content were observed at 24 h compared to the other time points. Previous studies have shown that Keap1 degradation likely takes place through the autophagy system,[25,26] unlike Nrf-2 which is regularly degraded by the

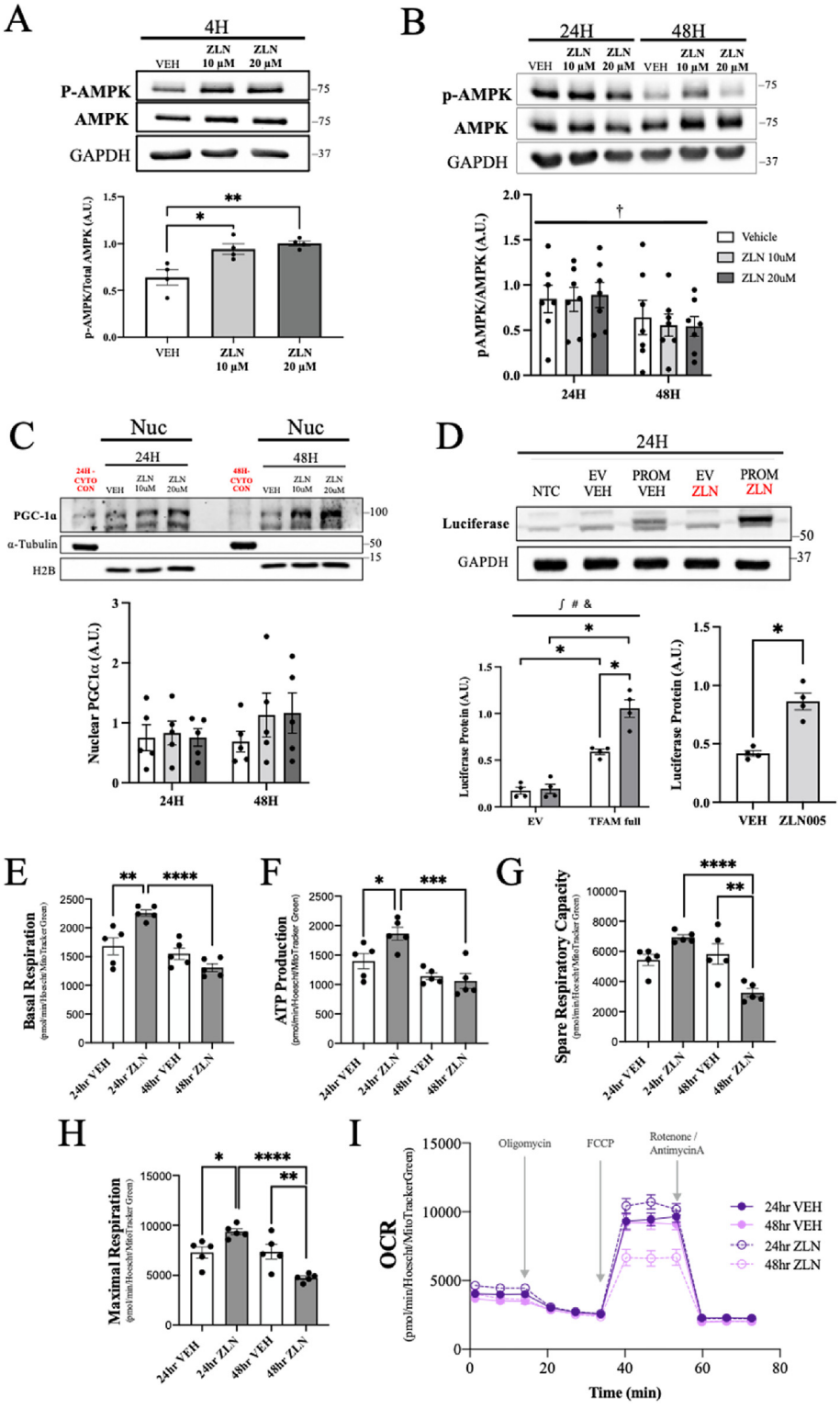

Fig. 6. Analysing the impact of ZLN005 on the drive for mitochondrial biogenesis and enhancing mitochondrial function. A, B: Western blot investigating whether the drive for biogenesis initiates with AMPK shown at 4 ($n = 4$), 24 ($n = 7$) and 48 h ($n = 7$) with the corresponding quantifications of pAMPK/AMPK ratio; One-way ANOVA, \$ $p < 0.05$, main effect of time. *$p < 0.05$, **$p < 0.01$, treatment vs. vehicle. C: Western blot investigating nuclear PGC-1α following ZLN treatment ($n = 5$) with the corresponding quantification of PGC-1α localization following 24 and 48 h of treatment. D: ZLN inhibits luciferase activity, thus requiring the assessment of TFAM promoter activity to be assessed by probing for luciferase protein content. Promoter-transfected cells treated with ZLN after 24 h were assessed ($n = 4$). Corresponding Luciferase quantification; two-way ANOVA, $\int p < 0.05$, main effect of treatment; $\#p < 0.05$, main effect of promoter; & $p < 0.05$, interaction effect between promoter and treatment; *$p < 0.05$, *t*-test between indicated conditions. Oxygen consumption rates during basal respiration (E), ATP production (F), spare respiratory capacity (G) and maximal respiration (H) using seahorse ($n = 6$). Representative oxygen consumption tracing (F). Seahorse data underwent a one-way ANOVA; *$p < 0.05$, **$p < 0.01$, ***$p < 0.001$, ****$p < 0.0001$. *AMPK,* AMP-activated Protein Kinase; *PGC-1α,* Peroxisome proliferator-activated receptor (PPAR) γ coactivator 1 alpha; *H2B,* Histone H2B; *TFAM,* Mitochondrial Transcription Factor A. *OCR,* Oxygen Consumption Rate. Values are represented as means ± *SEM*.

ubiquitin proteasome system. However, Nrf-2-mediated antioxidant activation has been reported to initiate autophagy[27] as well, which may account for the partial declines in Keap1 content 24 h post-induction with SFN. It is unclear whether this renders a positive feedback loop, where autophagy-mediated degradation of inactive Keap1 also results in further activation of nascent Nrf-2. However, SFN has been demonstrated to activate autophagy where p62 competes with Nrf-2-Keap1 binding,[28] suggesting a strong relationship between the antioxidant and autophagy systems as a result of SFN action.

Nrf-2 is a transcription factor that directly regulates the expression of antioxidant enzymes to promote the preservation of mitochondria. Thus, following Nrf-2 nuclear localization, we expected changes in the antioxidant enzymes NQO1 and HO-1. Consistent with the hypothesis surrounding the effect of time on upstream and downstream protein content, NQO1 increased in content starting at 24 h of treatment. Previous studies[29,30] have identified the role of NQO1 as a protective enzyme

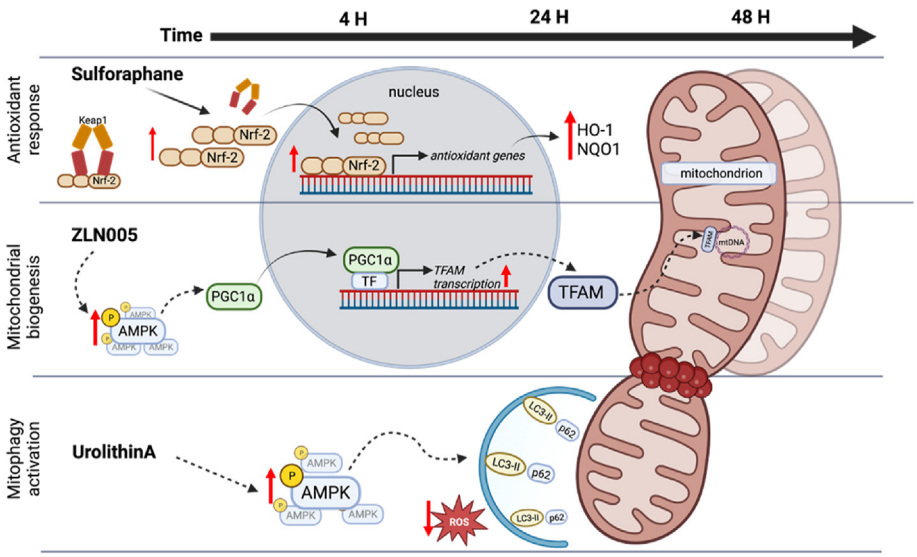

Fig. 7. Mechanisms and stimuli that contribute to mitochondrial turnover and homeostasis. Under homeostatic conditions, Nrf-2 is sequestered in the cytosol by its negative regulator Keap1.[7] Sulforaphane disrupts this interaction, leading to the accumulation and nuclear localization of Nrf-2 by 4 h.[7] Nrf-2 binds to ARE elements found upstream of antioxidant promoters HO-1 and NQO1,[7] resulting in protein changes by 24 h. These antioxidants mitigate excessive ROS, thereby preserving mitochondrial content and function by 48 h. ZLN005 induces AMPK activation by 4 h, and subsequent upregulation of TFAM transcription by 24 h. TFAM binds mitochondrial DNA to activate transcription and replication, thereby enhancing mitochondrial biogenesis. UrolithinA enhances AMPK activation by 4 h, resulting in the activation of mitophagy machinery and reduction in cellular ROS by 24 h. *Nrf-2*, Nuclear factor (erythroid-derived 2)-like 2. *Keap1*, Kelch-like ECH-associated protein. *HO-1*, Heme-Oxygenase-1. *NQO1*, Nicotinamide Quinone Oxidoreductase 1. *AMPK*, AMP-activated Protein Kinase. *TFAM*, Mitochondrial Transcription Factor A. *ROS*, Reactive Oxygen Species.

which adds complexity to "intrinsically disordered proteins" (IDP) that are regularly degraded by the 20S proteasomal system due to their intrinsic unfolded composition. PGC-1α has been identified as an IDP, and as a result, NQO1 in the presence of NADH can bind and allow the co-transcriptional regulator to bypass the proteasome and undergo the necessary posttranslational modifications that promote its nuclear localization and activity. While we currently do not show direct evidence to suggest that NQO1 carries out this protective function, we found that by 24 h mitochondrial respiration was enhanced which was followed by increased COX IV by 48 h, suggesting a crosstalk between the antioxidant and mitochondrial biogenesis mechanisms. Furthermore, it has been shown that Nuclear Respiratory Factors-1 (NRF1) and −2 (NRF2) contain promoter AREs which are recognized by Nrf-2.[31] Since NRFs are positive regulators of nuclear gene-encoding mitochondrial proteins (NuGEMPs),[1,32,33] it is possible that SFN-induced Nrf-2 activation may result in mitochondrial biogenesis via this mechanism.

Additionally, HO-1 has been reported to mediate many protective mechanisms, including mitochondrial quality control[34] and anti-inflammation,[35] which were reported in the heart and vasculature. The skeletal muscle-specific HO-1 knockout animal showed impairments in aerobic performance, shifting towards a glycolytic phenotype. Additional observations included reduced cross-sectional area due to increased muscle atrophy, as well as increased mitochondrial fragmentation and reduced citrate synthase activity, as an indication of mitochondrial dysfunction.[36] HO-1, in the context of skeletal muscle, sequesters free heme and prevents its release into the cytoplasm or even leakage into plasma following microtrauma. This action spares the potential for ferroptosis-induced lipid peroxidation. Interestingly, the response in HO-1 protein content came as early as 4 h of SFN treatment and was maintained at 24 and 48 h. This demonstrates that, while SFN increases in HO-1 content, it is possible that the early increase of this protein occurs through an Nrf-2/ARE-independent manner, the evidence for this is that when mutations in a repressor of the HO-1 gene, Bach1, were examined in an Nrf-2-null phenotype, these mice still showed increased HO-1 expression, suggesting that it can be reliant on other activators.[37] Our data clearly show that increased HO-1 content is dependent on SFN treatment, but further investigation is required to examine its relationship with Nrf-2-mediated transcription, its earlier expression, and its relevance to cytoprotection.

The important complement to organellular production is also its efficient removal via mitophagy, to sustain a consistently healthy mitochondrial phenotype. Urolithin A has been shown to induce mitophagy in an AMPK-dependent manner, followed by the induction of mitophagy-related proteins including LC3-II and p62, in *C. elegans*, C2C12 myoblasts, rodent models, and middle-aged and elderly human subjects.[11–15] However, some of these data remain unconvincing with respect to mitochondria-specific (mitophagy) flux,[11–15] an indicator of increased mitochondrial targeting for degradation. It is prudent to present strong data on this front to fortify the efficacy of UroA as a mitophagy activator. Beginning with whole cell examination, we observed increased phospho-AMPK after 4 h of treatment (Fig. 5A), despite previous findings after 24 h.[11] Further, while the downstream mitophagy markers p62 and LC3-II also increased significantly by 48 h, their change appeared modest compared to control levels in whole cells. Through co-treatment with BafA followed by mitochondrial isolation, we were able to showcase its ability to activate mitophagy as we observed increased LC3-II and p62 flux at 24 or at 48 h (Fig. 5B and C). Interestingly, this was accompanied by a reduction in cellular ROS by 24 h (Fig. 5D). While additional investigation is required to add to the efficacy of UroA, our data firmly support the fact that UroA increases mitophagy flux, which results in a reduction in cellular ROS.

As we have determined candidate molecules that enhance antioxidant capacity and mitophagy, we wished to include an agent that might directly contribute to mitochondrial biogenesis, thus covering each approach towards mitochondrial homeostasis. Data mining and consultation of the literature uncovered the small molecule, ZLN005.[16] It has been reported to activate the master regulator of mitochondrial biogenesis, PGC-1α, by facilitating its nuclear translocation through the upstream master regulator of cell metabolism, AMPK.[16] We acknowledge that ZLN and UroA have both been presented as activators of their relevant pathways through AMPK but identified differently as contributors to cellular metabolism. PGC-1α has been shown to regulate mitochondrial biogenesis, mitochondrial fission, and mitophagy activation.[1] Recent evidence has also shown that pools of AMPK bind to mitochondria directly as they modulate mitochondrial fate.[38] As a result, it is useful to investigate the effects of these AMPK activators on other mitochondria-related pathways to determine why they are recognized for one particular function or mechanism. In line with this mechanism, AMPK activation was observed at 4 h, with likely downstream consequences, which dissipated by 24 and 48 h (Fig. 6A and B).

While we used nuclear fractions after 4, 24, and 48 h of ZLN treatment, we were unable to establish its role as a PGC-1α activator within nuclear fractions. However, we used a promoter-reporter of TFAM, a known PGC-1α co-transcriptional target,[39] as a surrogate measure of an increased drive for mitochondrial biogenesis upstream, since PGC-1α coactivates NRF-1 on the TFAM promoter. There was a marked 2-fold

increase in luciferase content following a transient transfection with a TFAM promoter within a 24-h time point (Fig. 6D). We hope to continue fortifying the role of ZLN as an activator of mitochondrial biogenesis via PGC-1α by adding downstream mitochondrial markers resulting from TFAM transcription, such as COX subunit I.

5. Conclusion

Taken together, our results indicate that the agents SFN, UroA, and ZLN increase proteins affiliated with the three overarching mechanisms of mitochondrial turnover in a time-dependent manner. Early time points involve the activation of upstream mechanisms of action with respect to kinase phosphorylation, nuclear translocation, and transcriptional activity, whereas later time points represent the increased activity in their associated downstream markers (Fig. 7). Continued characterization of these agents in our *in vitro* model is required to sufficiently report on their specificity for mitochondrial biogenesis, mitophagy, or antioxidant capacity. Overall, this research sets the stage for future work that can illuminate their utility as preservers of mitochondrial health in skeletal muscle.

Funding

This work was supported by a grant from the Natural Science and Engineering Council (NSERC). Neushaw Moradi is a recipient of the Ontario Graduate Scholarship (OGS). Sabrina Champsi is a recipient of the NSERC Alexander Graham Bell Canada Graduate Scholarship-Master's (CGS-M). David A. Hood holds a Tier I Canada Research Chair in Cell Physiology.

Data availability

Data are available upon request from the authors.

CRediT authorship contribution statement

Neushaw Moradi: Writing – review & editing, Writing – original draft, Investigation, Conceptualization. **Sabrina Champsi:** Writing – review & editing, Writing – original draft, Investigation. **David A. Hood:** Writing – review & editing, Supervision, Methodology, Funding acquisition, Conceptualization.

Conflict of interest

David H. Hood is an Editorial Board Member for Sports Medicine and Health Science and was not involved in the editorial review or the decision to publish this article. The authors declare they have no financial interests/personal relationships that could have appeared to influence the work reported in this paper.

Acknowledgments

We would like to acknowledge Dr. Ashley Oliveira and Dr. Debasmita Bhattacharya for their expert advice and technical assistance.

References

1. Hood DA, Memme JM, Oliveira AN, Triolo M. Maintenance of skeletal muscle mitochondria in health, exercise, and aging. *Annu Rev Physiol*. 2019;81(1):19–41. https://doi.org/10.1146/annurev-physiol-020518-114310.
2. Ljubicic V, Hood DA. Diminished contraction-induced intracellular signaling towards mitochondrial biogenesis in aged skeletal muscle. *Aging Cell*. 2009;8(4):394–404. https://doi.org/10.1111/j.1474-9726.2009.00483.x.
3. Ljubicic V, Joseph A, Adhihetty PJ, et al. Molecular basis for an attenuated mitochondrial adaptive plasticity in aged skeletal muscle. *Aging*. 2009;1(9):818–830. https://doi.org/10.18632/aging.100083.
4. Hood DA, Uguccioni G, Vainshtein A, D'souza D. Mechanisms of exercise-induced mitochondrial biogenesis in skeletal muscle: implications for health and disease. *Compr Physiol*. 2011;1(3):1119–1134. https://doi.org/10.1002/cphy.c100074.
5. Chen C, Erlich AT, Hood DA. Role of Parkin and endurance training on mitochondrial turnover in skeletal muscle. *Skeletal Muscle*. 2018;8(1):10. https://doi.org/10.1186/s13395-018-0157-y.
6. Holloszy JO, Coyle EF. Adaptations of skeletal muscle to endurance exercise and their metabolic consequences. *J Appl Physiol Respir Environ Exerc Physiol*. 1984;56(4):831–838. https://doi.org/10.1152/jappl.1984.56.4.831.
7. Yamamoto M, Kensler TW, Motohashi H. The KEAP1-NRF2 system: a thiol-based sensor-effector apparatus for maintaining redox homeostasis. *Physiol Rev*. 2018;98(3):1169–1203. https://doi.org/10.1152/physrev.00023.2017.
8. Li D, Shao R, Wang N, et al. Sulforaphane activates a lysosome-dependent transcriptional program to mitigate oxidative stress. *Autophagy*. 2020;17(4):872–887. https://doi.org/10.1080/15548627.2020.1739442.
9. Malaguti M, Angeloni C, Garatachea N, et al. Sulforaphane treatment protects skeletal muscle against damage induced by exhaustive exercise in rats. *J Appl Physiol*. 2009;107(4):1028–1036. https://doi.org/10.1152/japplphysiol.00293.2009.
10. Moon JY, Kim DJ, Kim HS. Sulforaphane ameliorates serum starvation-induced muscle atrophy via activation of the Nrf2 pathway in cultured C2C12 cells. *Cell Biol Int*. 2020;44(9):1831–1839. https://doi.org/10.1002/cbin.11377.
11. Ryu D, Mouchiroud L, Andreux PA, et al. Urolithin A induces mitophagy and prolongs lifespan in C. elegans and increases muscle function in rodents. *Nat Med*. 2016;22(8):879–888. https://doi.org/10.1038/nm.4132.
12. Luan P, D'Amico D, Andreux PA, et al. Urolithin A improves muscle function by inducing mitophagy in muscular dystrophy. *Sci Transl Med*. 2021;13(588):eabb0319. https://doi.org/10.1126/scitranslmed.abb0319.
13. Andreux PA, Blanco-Bose W, Ryu D, et al. The mitophagy activator Urolithin A is safe and induces a molecular signature of improved mitochondrial and cellular health in humans. *Nat Metab*. 2019;1(6):595–603. https://doi.org/10.1038/s42255-019-0073-4.
14. Liu S, D'Amico D, Shankland E, et al. Effect of Urolithin A supplementation on muscle endurance and mitochondrial health in older adults. *JAMA Netw Open*. 2022;5(1):e2144279. https://doi.org/10.1001/jamanetworkopen.2021.44279.
15. D'Amico D, Olmer M, Fouassier AM. Urolithin A improves mitochondrial health, reduces cartilage degeneration, and alleviates pain in osteoarthritis. *Aging Cell*. 2022;21(8):e13662. https://doi.org/10.1111/acel.13662.
16. Zhang L, Zhou H, Fu Y, et al. Novel small-molecule PGC-1α transcriptional regulator with beneficial effects on diabetic db/db mice. *Diabetes*. 2013;62(4):1297–1307. https://doi.org/10.2337/db12-0703.
17. Liu Y, Bai H, Guo F, et al. PGC-1α activator ZLN005 promotes maturation of cardiomyocytes derived from human embryonic stem cells. *Aging*. 2020;12(8):7411–7430. https://doi.org/10.18632/aging.103088.
18. Russo M, Spagnuolo C, Russo GL, et al. Nrf2 targeting by sulforaphane: a potential therapy for cancer treatment. *Crit Rev Food Sci Nutr*. 2017;58(8):1391–1405. https://doi.org/10.1080/10408398.2016.1259983.
19. Bahn G, Park J, Yun UJ, et al. NRF2/ARE pathway negatively regulates BACE1 expression and ameliorates cognitive deficits in mouse Alzheimer's models. *Proc Natl Acad Sci USA*. 2019;116(25):12516–12523. https://doi.org/10.1073/pnas.1819541116.
20. Yan X, Shen Z, Yu D. Nrf2 contributes to the benefits of exercise interventions on age-related skeletal muscle disorder via regulating Drp1 stability and mitochondrial fission. *Free Radic Biol Med*. 2022;178:59–75. https://doi.org/10.1016/j.freeradbiomed.2021.11.030.
21. Lin J, Wu H, Tarr PT, et al. Transcriptional Co-activator PGC-1α drives the formation of slow-twitch muscle fibres. *Nature*. 2002;418(6899):797–801. https://doi.org/10.1038/nature00904.
22. Bhattacharya D, Oresajo O, Scimè A. P107 mediated mitochondrial function controls muscle stem cell proliferative fates. *Nat Commun*. 2021;12(1):5977. https://doi.org/10.1101/2020.09.29.317693.
23. Mauvezin C, Neufeld TP. Bafilomycin A1 disrupts autophagic flux by inhibiting both V-ATPase-dependent acidification and Ca-P60A/SERCA-dependent autophagosome-lysosome fusion. *Autophagy*. 2015;11(8):1437–1438. https://doi.org/10.1080/15548627.2015.1066957.
24. Piantadosi CA, Suliman HB. Redox regulation of mitochondrial biogenesis. *Free Radic Biol Med*. 2012;53(11):2043–2053. https://doi.org/10.1016/j.freeradbiomed.2012.09.014.
25. Collu-Marchese M, Shuen M, Pauly M, Saleem A, Hood DA. The regulation of mitochondrial transcription factor a (Tfam) expression during skeletal muscle cell differentiation. *Biosci Rep*. 2015;35(3):e00221. https://doi.org/10.1042/bsr20150073.
26. Jain A, Lamark T, Sjøttem E, et al. P62/SQSTM1 is a target gene for transcription factor NRF2 and creates a positive feedback loop by inducing antioxidant response element-driven gene transcription. *J Biol Chem*. 2010;285(29):22576–22591. https://doi.org/10.1074/jbc.m110.118976.
27. Taguchi K, Fujikawa N, Komatsu M. Keap1 degradation by autophagy for the maintenance of redox homeostasis. *Proc Natl Acad Sci USA*. 2012;109(34):13561–13566. https://doi.org/10.1073/pnas.1121572109.
28. Jiang T, Harder B, Rojo de la Vega M, Wong PK, Chapman E, Zhang DD. P62 links autophagy and Nrf2 signaling. *Free Radic Biol Med*. 2015;88(Pt B):199–204. https://doi.org/10.1016/j.freeradbiomed.2015.06.014.
29. Tsvetkov P, Adler J, Strobelt R, et al. NQO1 binds and supports SIRT1 function. *Front Pharmacol*. 2021;12:671929. https://doi.org/10.3389/fphar.2021.671929.

30. Adamovich Y, Shlomai A, Tsvetkov P. The protein level of PGC-1α, a key metabolic regulator, is controlled by NADH-NQO1. *Mol Cell Biol*. 2013;33(13):2603–2613. https://doi.org/10.1128/mcb.01672-12.
31. Piantadosi CA, Carraway MS, Babiker A, Suliman HB. Heme oxygenase-1 regulates cardiac mitochondrial biogenesis via nrf2-mediated transcriptional control of nuclear respiratory factor-1. *Circ Res*. 2008;103(11):1232–1240. https://doi.org/10.1161/01.res.0000338597.71702.ad.
32. Zhang Y, Uguccioni G, Ljubicic V, et al. Multiple signaling pathways regulate contractile activity-mediated PGC-1α gene expression and activity in skeletal muscle cells. *Phys Rep*. 2014;2(5):e12008. https://doi.org/10.14814/phy2.12008.
33. Chabi B, Ljubicic V, Menzies KJ, Huang JH, Saleem A, Hood DA. Mitochondrial function and apoptotic susceptibility in aging skeletal muscle. *Aging Cell*. 2008;7(1):2–12. https://doi.org/10.1111/j.1474-9726.2007.00347.x.
34. Hull TD, Boddu R, Guo L, et al. Heme oxygenase-1 regulates mitochondrial quality control in the heart. *JCI Insight*. 2016;1(2):e85817. https://doi.org/10.1172/jci.insight.85817.
35. Araujo JA, Zhang M, Yin F. Heme oxygenase-1, oxidation, inflammation, and atherosclerosis. *Front Pharmacol*. 2012;19(3):119. https://doi.org/10.3389/fphar.2012.00119.
36. Alves de Souza RW, Gallo D, Lee GR. Skeletal muscle heme oxygenase-1 activity regulates aerobic capacity. *SSRN Electron J*. 2020;35(3):109018. https://doi.org/10.2139/ssrn.3671735.
37. Gureev AP, Shaforostova EA, Popov VN. Regulation of mitochondrial biogenesis as a way for active longevity: interaction between the Nrf2 and PGC-1α signaling pathways. *Front Genet*. 2019;14(10):435. https://doi.org/10.3389/fgene.2019.00435.
38. Drake JC, Wilson RJ, Laker RC, et al. Mitochondria-localized AMPK responds to local energetics and contributes to exercise and energetic stress-induced mitophagy. *Proc Natl Acad Sci USA*. 2021;118(37):e2025932118. https://doi.org/10.1073/pnas.2025932118.
39. Jannig PR, Dumesic PA, Spiegelman BM, Ruas JL. SnapShot: regulation and biology of PGC-1α. *Cell*. 2022;185(8):1444–1444.e1. https://doi.org/10.1016/j.cell.2022.03.027.